Journal of Cancer Research and Clinical Oncology (2026) 152:192
https://doi.org/10.1007/s00432-026-06630-6

RESEARCH

Evaluation of novel targeted small-molecule therapeutics in desmoplastic small round cell tumor (DSRCT) cells

Anne Hahn[1,7] · Julia Hentschel[1,8] · Shifa Saleem[1,9] · Sabine Becker[1] · Thomas Liehr[2] · Andreas Schober[3] · Oliver H. Krämer[4] · Jürgen Sonnemann[1,5,6] · Christian Marx[3]

Received: 24 August 2026 / Accepted: 20 September 2026
© The Author(s) 2026

Abstract

Purpose Desmoplastic small round cell tumor (DSRCT) is an aggressive sarcoma associated with an extremely poor prognosis. This study evaluates the therapeutic potential of targeted, non-DNA-damaging small-molecule inhibitors in an in vitro DSRCT model.

Methods We characterized the genomic architecture of the JN-DSRCT-1 cell line using fluorescence in situ hybridization (FISH) and sequencing of the tumor suppressor *TP53*. In silico analysis was performed to identify shared vulnerabilities between DSRCT and Ewing sarcoma (ES). Using flow cytometry (assessing cell death, mitochondrial membrane potential loss, caspase–3 activity, and cell cycle distribution) and quantitative real-time PCR (qPCR), we systematically evaluated a small-molecule screening panel. The panel targeted chromatin acetylation (entinostat, vorinostat, tenovin-1), p53 pathway activity (RETRA, nutlin-3, RITA), receptor tyrosine kinases (imatinib), and transcription factor DNA-binding dynamics (mithramycin).

Results JN-DSRCT-1 cells exhibited complex aneuploidy, and we confirmed the presence of the pathognomonic balanced *EWSR1::WT1* translocation. Histone deacetylase inhibitors (entinostat, vorinostat) and nutlin-3 (an MDM2 antagonist) triggered robust intrinsic apoptosis and upregulated p53 target genes (p21, PUMA, and NOXA). Mithramycin demonstrated high cytotoxicity, whereas imatinib was ineffective. Pan-caspase inhibition using z-VAD-FMK rescued cells from entinostat-, vorinostat-, nutlin-3-, and mithramycin-induced death, but failed to protect against tenovin-1, RITA, or RETRA, indicating the activation of caspase-independent cell death pathways.

Conclusion DSRCT cells display high sensitivity to histone deacetylase inhibition, p53 pathway activation, and mithramycin. Among these, histone deacetylase inhibition alone or in combination with other small molecule drugs represents a particularly promising strategy for overcoming DSRCT cell survival.

✉ Christian Marx
christian.marx@tu-ilmenau.de

1 Department of Pediatric and Adolescent Medicine, Jena University Hospital, Friedrich Schiller University Jena, Jena, Germany

2 Institute of Human Genetics, Jena University Hospital, Friedrich Schiller University, Jena, Germany

3 Institute for Micro and Nanotechnologies (MacroNano®), Nano-Biosystem Technology, Ilmenau University of Technology, Ilmenau, Germany

4 Institute of Toxicology, University Medical Center, Johannes Gutenberg University Mainz, Mainz, Germany

5 Research Center Lobeda, Jena University Hospital, Friedrich Schiller University Jena, Jena, Germany

6 Comprehensive Cancer Center Central Germany (CCCG), Campus Jena, Jena, Germany

7 Present address: Faculty of Health, Medicine and Behavioural Sciences, Clem Jones Centre for Ageing Dementia Research, Queensland Brain Institute, The University of Queensland, Brisbane 4072, Australia

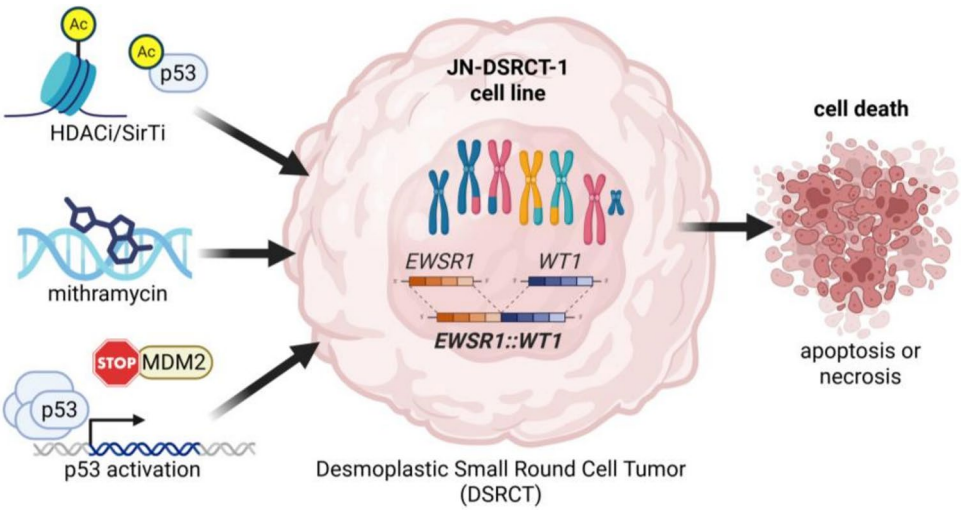
8 Present address: Institute of Human Genetics, University of Leipzig Medical Center, Leipzig, Germany

9 Present address: Medical Faculty, Martin Luther University Halle-Wittenberg, Halle (Saale), Germany

Published online: 03 October 2026

Graphical abstract

Therapeutic targeting and cell death modalities in JN-DSRCT-1 Cells. The JN-DSRCT-1 cell line serves as an in vitro model for desmoplastic small round cell tumor (DSRCT), featuring highly complex chromosomal aneuploidy alongside the pathognomonic reciprocal translocation t(11;22)(p13;q12) that generates the oncogenic EWSR1::WT1 fusion gene. The therapeutic potential of non-DNA-damaging small molecules was systematically profiled across three major molecular axes: (i) chromatin remodeling via histone deacetylase and sirtuin inhibitors (HDACi/SirTi), which promote hyperacetylation (Ac) of histones and non-histone proteins like p53; (ii) transcriptional interference via the DNA minor groove binder mithramycin; and (iii) direct p53 pathway activation through MDM2 inhibition. Exposure to these targeted compounds successfully bypasses oncogenic survival networks to trigger robust antitumor responses, ultimately driving tumor cell destruction through caspase-dependent apoptosis or caspase-independent necrosis. This figure was created using BioRender.com.



Keywords DSRCT · EWS-WT1 · HDAC · p53 · Targeted therapy · Cancer cell death

Abbreviations

AIF	Apoptosis-inducing factor
CNA	Copy number alterations
CDK	Cyclin dependent kinase
CDKN2A	Cyclin dependent kinase inhibitor 2A
CDKN2B	Cyclin dependent kinase inhibitor 2B
DSRCT	Desmoplastic small round cell tumor
EMA	European Medicines Agency
ES	Ewing sarcoma
EWSR1	Ewing Sarcoma Breakpoint Region 1
FISH	Fluorescence in situ hybridization
FDA	Food and Drug Administration
PDGFRA	Platelet-derived growth factor receptor alpha
HDAC	Histone deacetylase
HDACi	HDAC inhibitor
ΔΨm	Loss of mitochondrial transmembrane potential
MOMP	Mitochondrial outer membrane permeabilization
M-FISH	Multicolor-FISH
mt-p53	Mutant p53
NMPA	National medical products administration
NAD^+	Nicotinamide adenine dinucleotide
PMDA	Pharmaceuticals and Medical Devices Agency
PNETs	Primitive neuroectodermal tumors
PI	Propidium iodide
qPCR	Quantitative real-time PCR
SirT	Sirtuin
SirTi	SirT inhibitor
TKI	Tyrosine kinase inhibitor
VPA	Valproic acid
VCEP	Variant Curation Expert Panel
VEGF	Vascular endothelial growth factor
wt-p53	Wild-type p53
WT1	Wilms Tumor-1
WT	Wilms tumors
zVAD	Z-VAD-FMK

Introduction

Desmoplastic small round cell tumor (DSRCT) is a highly aggressive soft tissue sarcoma and, like Ewing sarcoma (ES), primitive neuroectodermal tumors (PNETs), and

Wilms tumors (WT), is classified as a round blue cell tumor (Hovsepyan et al. 2023). The disease was first described in 1989 by Gerald and Rosai (Gerald and Rosai 1989) and is relatively rare: only about 200 cases were documented in the following 20 years (Mello et al. 2021; Miwa et al. 2010). The cellular origin of the disease is unknown; as multiple tissue markers are expressed simultaneously. Biopsies show nests of small, round, undifferentiated cells in desmoplastic stroma (Hovsepyan et al. 2023). Male patients outnumber female patients by a factor of 4–5, and the mean age of patients at the time of diagnosis is between 19 and 27 years (Gedminas et al. 2020). Symptoms are rather non-specific and include weight loss, gastrointestinal disturbances, nausea, and abdominal pain (Hovsepyan et al. 2023). Despite great effort, the disease can be brought under chronic control only in individual cases. Treatment success depends heavily on the percentage of the tumors that can be surgically removed; cytoreductive surgery is often followed by intensive multi-agent chemotherapy and postoperative whole abdominopelvic radiotherapy (Hovsepyan et al. 2023; Mello et al. 2021). Median progression-free survival ranges between 4 and 21 months, and overall survival between 17 and 60 months, with the 5-year overall survival rate in the range of 10–20% (Hovsepyan et al. 2023).

The *EWSR1* (Ewing Sarcoma Breakpoint Region 1) gene encodes the RNA-binding protein EWS, a member of the TET (TLS/EWS/TAF15) protein family (Delattre et al. 1992; Sankar and Lessnick 2011). The molecular hallmark of DSRCT is the reciprocal chromosomal translocation t(11;22) (p13; q12), typically connecting *EWSR1* in intron 7–10 on chromosome 22 and, invariably, the exons 7 and 8 of *WT1* (Wilms Tumor-1) on chromosome 11, creating the *EWSR1::WT1* fusion gene (Gedminas et al. 2020; Hovsepyan et al. 2023; Mello et al. 2021). Thereby, this translocation results in a chimeric transcription factor EWS-WT1 that regulates genes involved in cell cycle progression, exocytosis, vascularization and tissue invasion, such as the platelet-derived growth factor receptor alpha *(PDGFRA)*, and the vascular endothelial growth factor (*VEGF*) (Gedminas et al. 2020; Mello et al. 2021).

Dysregulation of histone deacetylases (HDACs) is a common feature in many cancers (Liang et al. 2023; Thomas et al. 2011). HDACs are phylogenetically divided into five classes: Classical HDACs are zinc-dependent metalloenzymes divided into classes I, II, and IV based on structural homology, expression patterns, and cellular localization (Seto and Yoshida 2014). Class I HDACs are ubiquitously expressed, nuclear-localized enzymes that deacetylate core histone proteins and repress transcription. Class II (subdivided into IIa and IIb) and class IV (only HDAC11) enzymes exhibit tissue-specific expression, dynamically shuttle or reside in the cytoplasm, and frequently target non-histone substrates (Seto and Yoshida 2014; Thomas et al. 2011). In contrast, sirtuins (SirT1–7) belonging to HDAC class III, are structurally distinct enzymes that require nicotinamide adenine dinucleotide (NAD^+) as a cofactor, directly linking their epigenetic and metabolic activities to the nutritional state of the cell (Wu et al. 2022). HDAC and SirT inhibitors (HDACi/SirTi) can shift gene expression toward differentiation or apoptosis by increasing the acetylation both of histones and non-histone proteins, including p53 (Koppenhafer et al. 2025; Liang et al. 2023; Marx et al. 2018; Sonnemann et al. 2014), and are valuable therapeutic options beyond traditional chemotherapeutic regimens. Within a clinical study cohort evaluating *EWSR1*-rearranged round cell sarcomas (Dermawan et al. 2024), comprising 173 ES (harboring the *EWSR1::FLI1* or *EWSR1::ERG* fusion-oncogene) and 104 DSRCT cases (harboring the *EWSR1::WT1* fusion-oncogene), *ARID1A* mutations were noted in DSRCT but not in ES (in silico analysis of this cohort is included in the following sections of this study). The ARID1A protein interacts with the SWI/SNF protein complex to control chromatin structure, promotor accessibility and gene expressions; its mutations cause chromosomal alterations and cancer predisposition (Fontana et al. 2023; Fukumoto et al. 2018b). We and others have shown the effectiveness of chromatin-remodeling HDACi/SirTi in various cancer entities including ES (Koppenhafer et al. 2025; Marx et al. 2018; Sonnemann et al. 2014), which thus might also be useful for DSRCT.

Another exploitable weakness of DSRCT as of ES might be p53 upstream and downstream pathways, since *TP53* is found mutated in both tumors (Dermawan et al. 2024). We previously showed that activating p53 pathways offers promising therapeutic options for ES (Sonnemann et al. 2015, 2011), that might translate to the treatment of DSRCT cells. Inhibition of the EWS-WT1 fusion or its downstream targets is a major focus in DSRCT research (Boulay et al. 2024; Kawai-Kawachi et al. 2025). The tyrosine kinase inhibitor (TKI) imatinib is known to block BCR-ABL, c-Kit, and PDGFRA (Corless et al. 2005; Mello et al. 2021) drivers of cell cycle progression. Likewise, mithramycin, which is a DNA minor groove binding antibiotic, is known to impair EWS-FLI-mediated transcription in ES (Kaufman et al. 2026; Portugal 2024); both may influence DSRCT viability.

The objective of this study is to evaluate the effects of the HDACi entinostat, vorinostat, valproic acid, the SirTi tenovin-1, the p53 activity modulators RETRA, RITA, and nutlin-3, and of mithramycin on JN-DSRCT-1 cells. We utilized flow cytometry to measure propidium iodide (PI) uptake, the loss of mitochondrial transmembrane potential ($\Delta\Psi_m$) and caspase−3 activity as markers of mitochondrial damage and apoptosis. Additionally, p53 target gene mRNA

expression and cell cycle analysis are employed to elucidate the underlying molecular mechanisms of these compounds in DSRCT.

Materials and methods

Cell culture

The JN-DSRCT-1 cell line was established in 2002 by Nishio et al. (2002) and was originally derived from a tumor of a 7-year-old male patient. The fusion site of the two genes connects the *EWSR1* exon 10 and exon 8 of *WT1* (Nishio et al. 2002). JN-DSRCT-1 cells were a gift of Dr. Sean-Bong Lee (Tulane Cancer Center, LA, USA) and were maintained in conditioned medium: 1:1 mixture of DMEM and Ham's F12 medium (Lonza Group, Basel, Switzerland) supplemented with 10% fetal calf serum, 100 units/ml penicillin G sodium and 100 µg/ml streptomycin sulfate (Gibco/Invitrogen, Karlsruhe, Germany). They were cultivated at 37 °C in a humidified 5% CO_2 incubator and routinely passaged when 90% confluent.

Treatment of cells

Cells were seeded 24 h prior to drug exposure in tissue culture plates and treated for 24 h (qPCR) and 48 h (all other assays) with imatinib (PKC Pharmaceuticals, Woburn, MA, USA), mithramycin (PanReac/AppliChem, Darmstadt, Germany), vorinostat, entinostat, nutlin-3 (Alexis Biochemicals/Enzo Life Sciences, Lörrach, Germany), valproic acid (Sigma-Aldrich/Merck, Taufkirchen, Germany), RETRA (Tocris Bioscience, Bristol, UK), tenovin-1 or RITA (Cayman Chemical, Ann Arbor, MI, USA). If cells were treated additionally with the pan-caspase inhibitor z-VAD-FMK (zVAD; Alexis Biochemicals), the latter was added 1 h prior to treatment with other drugs.

Flow cytometric analysis of cell death and the loss of mitochondrial transmembrane potential ($\Delta\Psi_m$)

Analyses were done as previously described in (Marx-Blümel et al. 2017).

Caspase−3 activity

Analyses were done as previously described in (Marx-Blümel et al. 2017).

Cell cycle analysis

Analyses were done as previously described in (Gschwind et al. 2022).

PCR Analysis of the EWS-FLI1 fusion gene

Analysis of EWS-WT1 expression were done as previously described in (Nishio et al. 2002).

Fluorescence in situ hybridization (FISH)

FISH was done on chromosome preparations of the cell line JN-DSRCT-1. Chromosomes were prepared according to standard procedures (Weise and Liehr 2026). 20 metaphases, and where appropriate, also 20 interphase cells were evaluated per probe set applied. The presence of an *EWSR1* and a *WT1* gene rearrangement was checked using the commercially available probe sets ZytoLight SPEC EWSR1 Dual Color Break Apart Probe and ZytoLight SPEC WT1 Dual Color Break Apart Probe (Zytovision, Bremerhaven, Germany). A gene fusion *EWSR1* and FLI1 was confirmed using ZytoLight SPEC EWSR1/FLI1 Tricheck Probe (Zytovision, Bremerhaven, Germany). FISH was done as previously reported (Liehr 2026a).

Multicolor-FISH (M-FISH) analysis using a homemade whole chromosome painting probes (Liehr 2026b) was applied to resolve the complex karyotype of the cell line. As previously reported karyotype was determined by combining M-FISH data with inverted DAPI (4′,6-diamidino-2-phenylindole) banding.

TP53 sequencing

Sequencing was done using as described previously (Hentschel et al. 2011). Analysis of the *TP53* gene in JN-DSRCT-1 cells was done using JSI medical systems GmbH (Kippenheim, Germany).

Quantitative real-time PCR (qPCR)

Total RNA was isolated using Peqgold Total RNA Kit including DNase digestion (Peqlab, Erlangen, Germany). RNA was transcribed into cDNA using Omniscript (Qiagen, Hilden, Germany). Quantitative PCR was performed using the Applied Biosystems 7900HT real-time PCR system. Expression levels of p21 (*CDKN1A*) were normalized to 18S rRNA. Reactions were done in duplicate using Applied Biosystems (Darmstadt, Germany) Gene Expression Assays (18 s rRNA: Hs99999901_s1, *CDKN1A*: Hs00355782_m1, *PMAIP1*: Hs00560402_m1, *BBC3*: Hs00248075_m1) and Universal PCR Master Mix. All procedures were performed

according to the manufacturer's protocols. The relative gene expressions were calculated by the $2^{(\Delta\Delta Ct)}$ method.

In silico genomic analysis using cBioPortal

To explore the genomic and molecular differences between DSRCT and ES, in silico analysis was performed using the cBioPortal for Cancer Genomics framework (http://www.cbioportal.org). Genomic data were obtained from a publicly available Memorial Sloan Kettering Cancer Center cohort evaluating EWSR1-rearranged round cell sarcomas (Dermawan et al. 2024), which comprises 173 ES and 104 DSRCT cases. Clinical features, copy number alterations (CNA), mutations and structural variants of genes were compared between the two specific tumor entities using cBioPortal's integrated exploration tools.

Data analysis

Statistical significance of differences between experimental groups was calculated using a two-tailed Student's t-test using Microsoft 365 Excel; * = $p < 0.05$, ** = $p < 0.01$, *** = $p < 0.001$.

Results

Molecular cytogenetic characterization of the JN-DSRCT-1 cell line

Since its establishment in 2002 by Nishio et al. (2002), the JN-DSRCT-1 cell line has been used in research frequently, but the chromosomal complexity of these cells is still not fully understood. The *EWSR1::WT1* gene fusion serves as an exclusive diagnostic hallmark for the vast majority of DSRCT. We confirmed the fusion between *EWSR1* and *WT1* in the JN-DSRCT-1 cell line by PCR (Suppl. Fig. S1A). LNCaP cells, which were used as control, did not show a *EWSW1::WT1* PCR product, as expected. We further characterized the chromosomal complexity in JN-DSRCT-1 cells using cytogenetics and fluorescence in situ hybridization (FISH) (Suppl. Fig. S1B, C, S2 and S3). Inverted DAPI-banding and molecular cytogenetic analysis confirmed the presence of the diagnostic reciprocal translocation t(11;22)(p13;q12). This rearrangement results in the characteristic *EWSR1::WT1* gene fusion. Due to clonal evolution and numerical duplication, this locus is represented by a single derivative chromosome 11 (der(11)t(11;22)) alongside a duplicated derivative chromosome 22 (+der(22)t(11;22)(p13;q12)), effectively yielding two copies of the der(22) fusion marker (Suppl. Fig. S1B, C and S2). Of note, we did not detect the *EWSR1::FLI1* fusion gene in JN-DSRCT-1 cells by FISH (Suppl. Fig S3).

Karyotypic analysis of the JN-DSRCT-1 cell line demonstrates a highly complex chromosomal architecture characterized by pronounced aneuploidy (chromosome count ranging from 45 to 49) and presence of multiple rearrangements (Suppl. Fig. S1B, C and S2). The karyotype could be determined as 45~49, XY, +der(5)t(5;8)(p15;p21), der(8)t(1;8)(p36;p11.1), der(11)t(11;22)(p13;q12), der(11)(11pter->11q12::8p21->8p11.1::1q12->1qter), t(17;21)(p11;p11), der(22)t(11;22)(p13;q12), +der(22)t(11;22)(p13;q12)[cp20]. Overall, these rearrangements lead to partial trisomy for chromosomes 1 and 5, 11 and 22 paired with an 8q terminal fragment, der(8), and monosomy 11 (−11). Additionally, there is a balanced rearrangement between chromosomes 17 and 21 (der(17)t(17;21) and der(21)t(17;21)) not involving the 17p13 locus according to the FISH data, the site of *TP53*, which encodes the tumor suppressor p53 (van Kampen et al. 2025). The *TP53* status of the JN-DSRCT-1 cell line was further characterized by sequencing revealing two single nucleotide variants in this gene (Suppl. Fig. S4). The proline 72 to arginine substitution (c.215C>G, p.(Pro72Arg)) of p53 is already known to be non-pathogenic (De Souza et al. 2021). The second variant results in a heterozygous substitution of leucine 43 with phenylalanine (c.129G>C, p.(Leu43Phe)). This variant has an allele frequency of 0.00018% in the general population referring to the gnomAD database (v4.1.1; https://gnomad.broadinstitute.org/). Compared to wild-type p53 (wt-p53), p53 Leu-43Phe mutants showed comparable expression levels of p53 target genes and of p21 protein following radiation in a recent publication (Abreu et al. 2024), indicating that the p53 Leu43Phe variant is functional. Therefore, this variant can be classified as likely benign according to the ClinGen VCEP (Variant Curation Expert Panel) gene-specific recommendations (https://clinicalgenome.org/affiliation/50013). Consequently, the JN-DSRCT-1 cell line serves as a validated, genetically authentic model of DSRCT, including chromosomal aberrations, and offers a suitable platform for investigating novel targeted therapeutics.

In silico analysis of druggable targets

To explore druggable vulnerabilities in DSRCT, we performed an in silico analysis using the cBioPortal framework based on the genomic data from a published clinical study cohort evaluating *EWSR1*-rearranged round cell sarcomas (Dermawan et al. 2024), comprising 173 ES and 104 DSRCT cases. In silico analysis of this cohort revealed that in both ES and DSRCT the genes most frequently affected by copy number alterations (CNA) were *cyclin dependent kinase inhibitor 2A* (*CDKN2A*) and *2B* (*CDKN2B*) (Fig. 1A

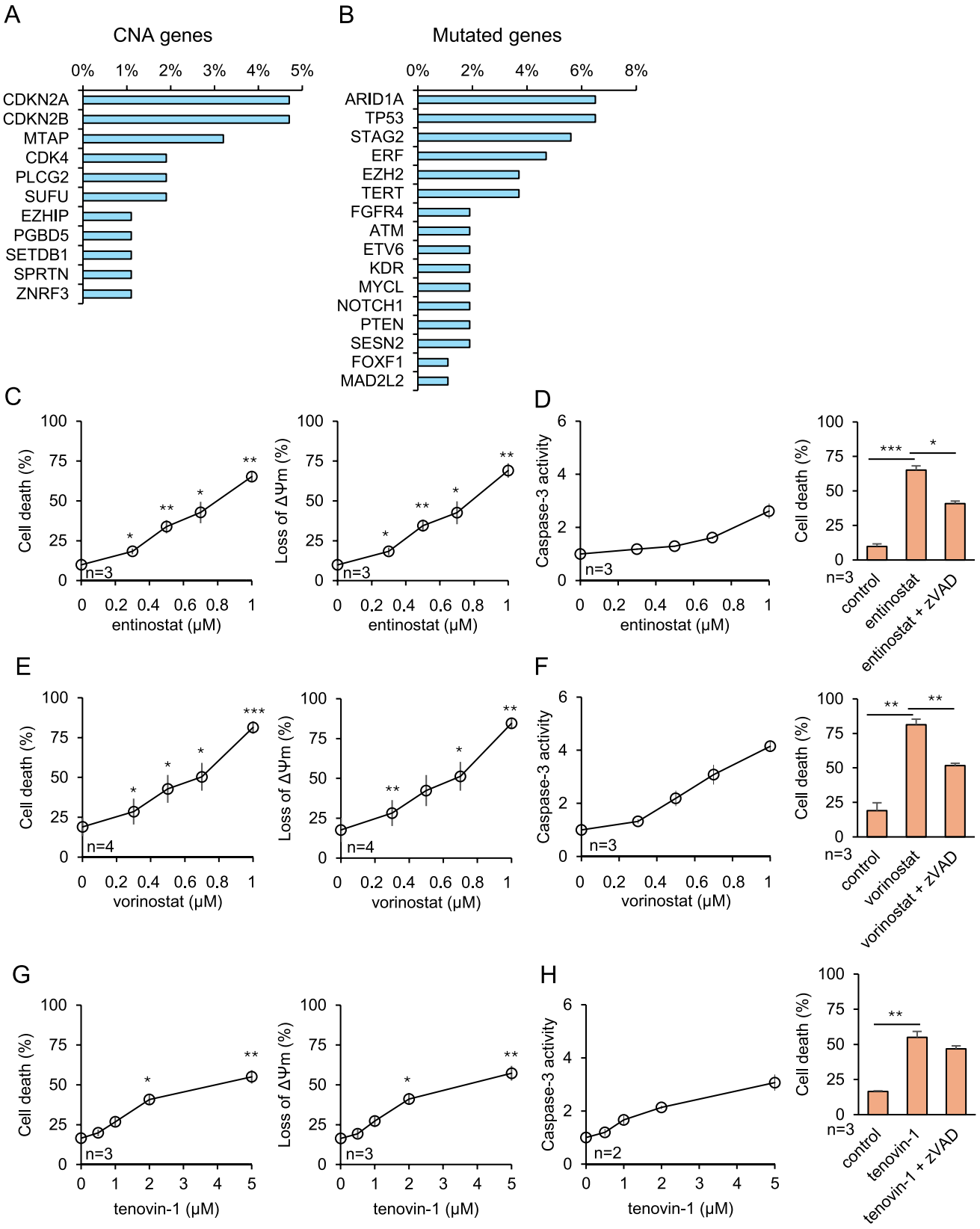

A
CNA genes
0% 1% 2% 3% 4% 5%
CDKN2A
CDKN2B
MTAP
CDK4
PLCG2
SUFU
EZHIP
PGBD5
SETDB1
SPRTN
ZNRF3
B
Mutated genes
0% 2% 4% 6% 8%
ARID1A
TP53
STAG2
ERF
EZH2
TERT
FGFR4
ATM
ETV6
KDR
MYCL
NOTCH1
PTEN
SESN2
FOXF1
MAD2L2
C
Cell death (%)
Loss of ΔΨm (%)
entinostat (μM)
n=3
D
Caspase-3 activity
Cell death (%)
control
entinostat
entinostat + zVAD
E
vorinostat (μM)
n=4
F
vorinostat
vorinostat + zVAD
G
tenovin-1 (μM)
H
n=2
tenovin-1
tenovin-1 + zVAD

Fig. 1 In silico characterization and cytotoxic response of JN-DSRCT-1 cells to HDACi. **A**, **B** In silico analysis was performed using the cBioPortal for Cancer Genomics framework based on the genomic data from a published Memorial Sloan Kettering Cancer Center clinical study cohort evaluating *EWSR1*-rearranged round cell sarcomas. Data for DSRCT patients is presented here as: **A** frequency of copy number alteration (CNA) variant genes; **B** frequency of mutated genes, highlighting somatic mutations. **C**–**H** Flow cytometric analyses of concentration-dependent cell death profiles, loss of mitochondrial membrane potential ($\Delta\Psi_m$), and caspase−3 enzymatic activity assays following 48 h treatment with: 0.3–1 µM entinostat (**C**, **D**), 0.3–1 µM vorinostat (**E**, **F**) and 0.5–5 µM tenovin-1 (**G**, **H**). Right-hand bar graphs illustrate the rescue effect on cell death when the highest applied concentration was combined with 20 µM of the pan-caspase inhibitor zVAD. Data are represented as mean ±SEM; the number of replicates is included in the figure. Statistical significance is designated as: * $p < 0.05$, ** $p < 0.01$, *** $p < 0.001$

and S5A). *CDKN2A,* encoding $p14^{ARF}$ and $p16^{INK4A}$, respectively, and *CDKN2B,* encoding $p15^{INK4B}$, regulate cell cycle progression via interaction with cyclin dependent kinases (CDKs) (Danishevich et al. 2023; Xia et al. 2021). The genomic architecture of JN-DSRCT-1 cells, however, showed a different set of CNAs (see above) and the *CDKN2A/B* locus (9p21 (Campa et al. 2016)) was copy-number neutral and structurally intact. Although rare, *TP53* and *STAG2* mutations, together with *CDKN2A* alterations are well described in ES patients and connected to a poor prognosis (Crompton et al. 2014; Tirode et al. 2014). Mirroring this, *TP53* and *STAG2* were among the mutated genes in both DSRCT and ES (Fig. 1B and S5B). The *TP53* sequencing of JN-DSRCT-1 cells confirms this (Suppl. Fig. S4). Thus, modulating p53 pathway activity might be a promising therapeutic approach for DSRCTs.

Interestingly, DSRCT patients have, among other genes, the highest mutation frequency in *ARID1A*, which is not common in ES (Fig. 1B and S5B). ARID1A belongs to the chromatin regulatory proteins and is mutated in about 10% of all human tumors of various origin (Fontana et al. 2023). In the JN-DSRCT-1 cell line, the *ARID1A* locus (1p36.11) is subject to a copy number gain, effectively present in three copies due to the partial trisomy of chromosome 1, and spatial relocation of chromosome 1, with one of those copies sitting on a structurally abnormal chromosome 8 (der(8)(1pter->1p11::8p12->8q21.3::8p22->8pter). Because the breakpoint for this translocation occurred at 1p11, the coding sequence of *ARID1A* itself is most likely intact. *ARID1A* mutations are connected to chromosomal alterations (Fontana et al. 2023; Fukumoto et al. 2018b) and might be a weakness of DSRC tumors.

Taken together, in silico analysis highlighted many overlapping gene mutations/alterations between ES and DSRCT patients, indicating that effective anti-ES therapies might also show promise in the treatment of DSRCT patients. We therefore aimed to evaluate the effects of a set of HDACi and SirTi, and of p53 pathway activity modulators, side by side with imatinib and mithramycin in a small molecule drug screening approach on JN-DSRCT-1 cells.

Experimental evaluation of entinostat in JN-DSRCT-1 cells

To determine the effectiveness of the class I/class IV HDACi entinostat (MS-275) (Thomas et al. 2011), PI uptake as marker for cell death was measured by flow cytometry. Unless specified otherwise, JN-DSRCT-1 cells were exposed to all small molecule agents for 48 h prior to analysis throughout. A narrow concentration gradient was trialed, causing a clear and significant concentration-dependent increase in cell death (65.2% at 1 µM) (Fig. 1C). The loss of $\Delta\Psi_m$ is a crucial event in intrinsic apoptosis execution and typically precedes large-scale genomic DNA fragmentation (Zamzami et al. 1995); it triggers the release of cytochrome c into the cytosol, initiating the downstream caspase cascade (Dho et al. 2025). The loss of $\Delta\Psi_m$ was assessed by flow cytometric using DiOC6(3) that ceases to accumulate in mitochondria of cells undergoing apoptosis. Increasing entinostat concentrations led to a significant and progressive $\Delta\Psi_m$ loss (69.1% at 1 µM) (Fig. 1C). The enzymatic activity of caspase−3, which we measured using the fluorogenic substrate Ac-DEVD-AMC, increased up to 2.6-fold relative to untreated cells (at 1 µM) (Fig. 1D). To further characterize its mechanism of action and delineate the role of caspase-dependent cell death, entinostat was combined with the pan-caspase inhibitor zVAD, which significantly reduced cell death by 24.3% (Fig. 1D), but had negligible impact on $\Delta\Psi_m$ loss (Suppl. Fig. S6A). This observation matches the classical model where the upstream mitochondrial outer membrane permeabilization (MOMP) occurs independently, or upstream of, effector caspase activity (Tait and Green 2008).

Evaluation of further HDACi therapeutics

To contextualize the effectiveness of entinostat, other HDACi/SirTi were evaluated under identical experimental conditions. The class I, II and IV HDACi vorinostat (SAHA) (Thomas et al. 2011) induced a significant, concentration-dependent increase in cell death (81.4% at 1 µM) and loss of $\Delta\Psi_m$ (84.6% at 1 µM) (Fig. 1E). Congruently, 1 µM vorinostat stimulated a 4-fold increase in caspase−3 activation; co-treatment with zVAD significantly reduced total cell death by 29.8%, with only marginal effects on the loss of $\Delta\Psi_m$ (Fig. 1F and S6A). The spot-check analysis of the class I and II HDACi valproic acid (VPA) (Thomas et al. 2011) confirmed the effectiveness of HDACi in JN-DSRCT-1 cells (Suppl. Fig. S6B-C). VPA induced a significant concentration-dependent increase in cell death (63.7% at 2 mM) and

loss of $\Delta\Psi_m$ (67.2% at 2 mM), which was accompanied by a 4.5-fold increase in caspase−3 activation (at 2 mM).

Finally, we tested class III HDACi (SirTi) to find the most relevant HDAC class in JN-DSRCT-1 cells. Sirtuins can deacetylate p53, thereby suppressing its pro-apoptotic function. This halts transition into senescence, while control mechanisms of cell cycle progression are simultaneously disabled (Marx et al. 2018). The SirT1/2 inhibitor tenovin-1 displayed a significant concentration–response effect; however, total cytotoxicity plateaued at 5 µM (55% cell death and 57.3% $\Delta\Psi_m$ loss at 5 µM) (Fig. 1G). Saturation kinetics of tenovin-1 beginning at 3 µM have been revealed in previous screenings in various ES cell lines (Marx et al. 2018). Upon exposure to 5 µM tenovin-1, caspase−3 activity rose 5-fold, however, co-treatment with zVAD failed to reduce cell death and $\Delta\Psi_m$ loss (Fig. 1H and S6A), indicating that tenovin-1-mediated cytotoxicity does not rely on caspase activation in JN-DSRCT-1 cells.

Restoring p53 pathway activity as therapeutic option

Tenovin-1 protects p53 from deacetylation and degradation, increasing its activity primarily in cells with wt-p53 (Lain et al. 2008; Marx et al. 2018; Sonnemann et al. 2014). (Re)activation of p53 and its downstream signaling is a key strategy for inducing apoptosis in malignant cells. This is often achieved by disrupting the inhibitory interaction of MDM2 with p53 (Wang et al. 2023). P63 and p73, members of the p53 family, have partial functional redundancy with p53. Some p53 mutants (mt-p53) lack tumor-suppressive properties, but interact with and sequester p73 and p63 (Klein et al. 2021; Wolf et al. 2018). The compound RETRA is designed to minimize the inhibitory effects of mt-p53 on p73, thereby restoring tumor-suppressive pathways in mt-p53 cells (Kravchenko et al. 2008; Sonnemann et al. 2015). The concentrations of RETRA tested in this screen displayed moderate anti-tumor effectiveness, with overall cell death of 28.5% and $\Delta\Psi_m$ loss in 30.8% of cells, both plateauing at 10 µM (Fig. 2A). Caspase−3 activation (1.4-fold at 10 µM) was weak compared to other compounds and co-treatment with zVAD yielded no significant reduction in cell death and $\Delta\Psi_m$ loss (Fig. 2B and S6D).

Nutlin-3 (4,5-dihydroimidazole), an MDM2 antagonist causing the stabilization and activation of p53 (Shen and Maki 2011), has a significant apoptotic influence on ES cell lines (Sonnemann et al. 2011). In our present small-molecule screen, nutlin-3 proved to be a highly potent agent, inducing up to 72.5% cell death and 71.8% $\Delta\Psi_m$ loss in JN-DSRCT-1 cells at low micromolar concentrations (5 µM) (Fig. 2C). This correlated with a strong 4.6-fold induction of caspase−3 activity; combining nutlin-3 with zVAD reduced cell death by 18.3% and the loss of $\Delta\Psi_m$ by 8.2% (Fig. 2D and S6D).

The molecule RITA inhibits the interaction of MDM2 and MDMX with wt-p53 or mt-p53 and only moderately affects non-malignant cells (Burmakin et al. 2013; Zhan et al. 2022). RITA demonstrated potency at nanomolar concentrations, inducing a concentration-dependent response that plateaued at 100 nM (45.8% cell death, 48.7% $\Delta\Psi_m$ loss and a 5.4-fold caspase−3 activation) (Fig. 2E, F). Co-treatment with zVAD failed to reduce cell death and $\Delta\Psi_m$ loss (Fig. 2F and S6D), indicating that RITA's primary mechanism of cell death is driven by alternative, caspase-independent pathways.

Comparative evaluation of alternative therapeutic agents

We asked if other therapeutics beyond chromatin remodeling and p53 activation would be effective in JN-DSRCT-1 cells. Mithramycin, shown to be very effective in ES (Kaufman et al. 2026; Portugal 2024), emerged as one of the most potent cytotoxic agents in our experimental panel. At just 50 nM, it triggered 80.2% cell death, $\Delta\Psi_m$ loss in 85.7% of cells (Fig. 2G) and a 5.4-fold caspase−3 activation (Fig. 2H). Co-treatment with zVAD reduced total cell death by 14% (Fig. 2H), while providing only mild reduction of $\Delta\Psi_m$ loss (Suppl. Fig. S6F). In contrast, the TKI imatinib demonstrated no meaningful therapeutic effectiveness against JN-DSRCT-1 cells. Across all evaluated concentrations, the fraction of dead cells and of cells exhibiting a loss of $\Delta\Psi_m$ remained at a baseline level of 10–15% (Suppl. Fig. S6E). We therefore discontinued the use of imatinib in this screen.

Analyses of cell cycle profiles and gene expression after HDACi treatment

P53 is a primary upstream regulator of caspase activation, DNA repair, and cell cycle arrest (Dho et al. 2025; Sullivan et al. 2018; Wang et al. 2023). Thus, we speculated that JN-DSRCT-1 cells might undergo cell cycle perturbations following treatments within this small-molecule screening panel. Cells were analyzed via flow cytometry-based quantitative DNA content profiling, which identified four distinct populations: sub-G1 (fragmented DNA, indicative for apoptosis), G1 (2n DNA content), S (replicating DNA), and G2/M-phase (4n DNA content, prior to cell division). In untreated conditions, most cells reside in G1-phase (Fig. 3). With increasing entinostat concentrations, accumulation of cells in the sub-G1 fraction occurred (Fig. 3A); the percentage of cells remaining in the G1-phase remained largely stable. Concurrently, S-phase and G2/M-phase populations

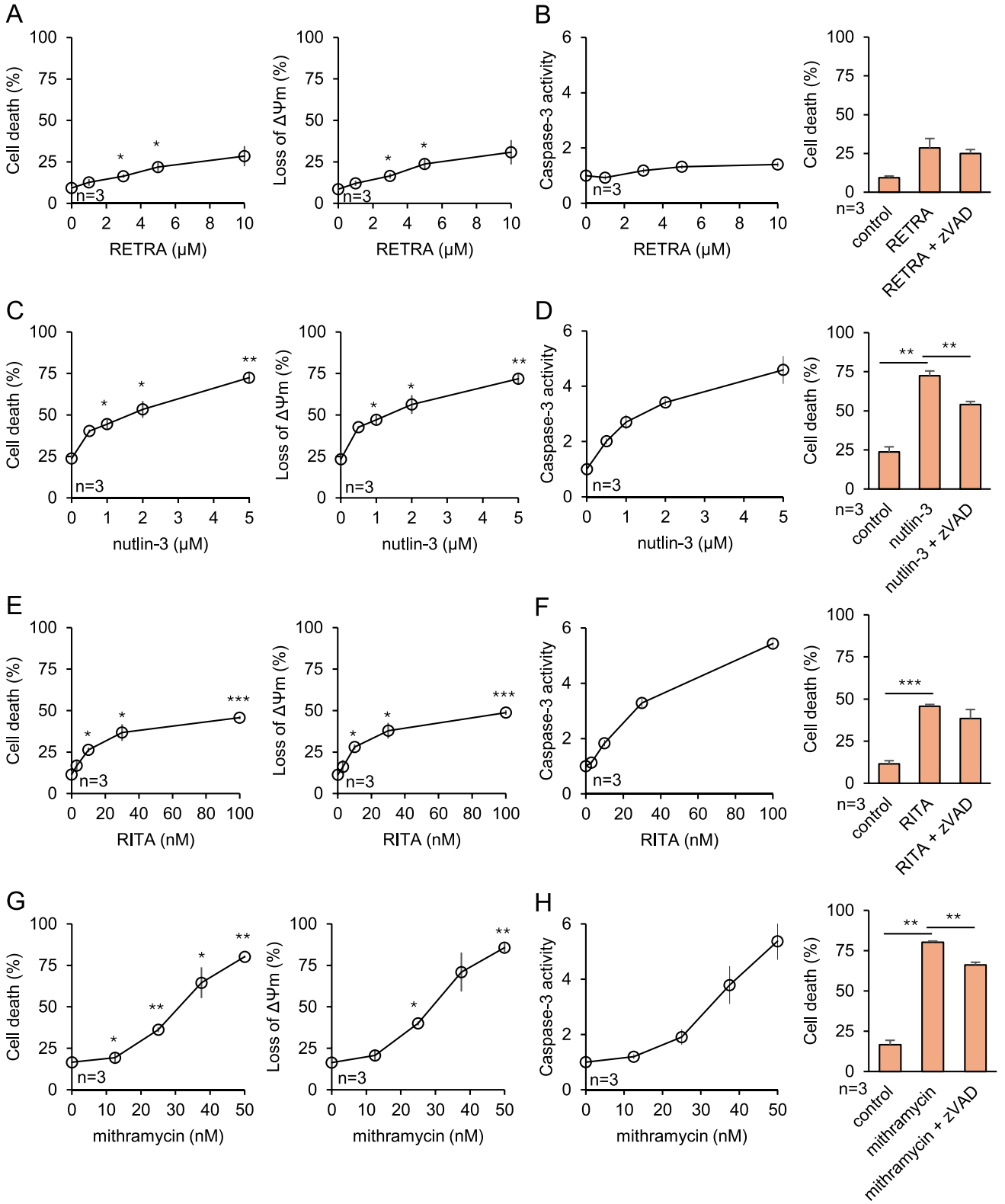


Fig. 2 Assessment of small-molecule induced apoptosis via p53 pathway activation or mithramycin. **A**–**H** Flow cytometric analyses of concentration-dependent cell death profiles, loss of $\Delta\Psi_m$, and caspase−3 enzymatic activity assays following 48 h treatment with: 1–10 µM RETRA (**A**, **B**), 0.5–5.0 µM nutlin-3 (**C**, **D**), 3–100 nM RITA (**E**, **F**) and 12.5–50.0 nM mithramycin (**G**, **H**). Right-hand bar graphs illustrate the rescue effect on cell death when the highest applied concentration was combined with 20 µM of the pan-caspase inhibitor zVAD. Data are represented as mean ±SEM; the number of replicates is given within the figure. Statistical significance is designated as: * $p < 0.05$, ** $p < 0.01$, *** $p < 0.001$

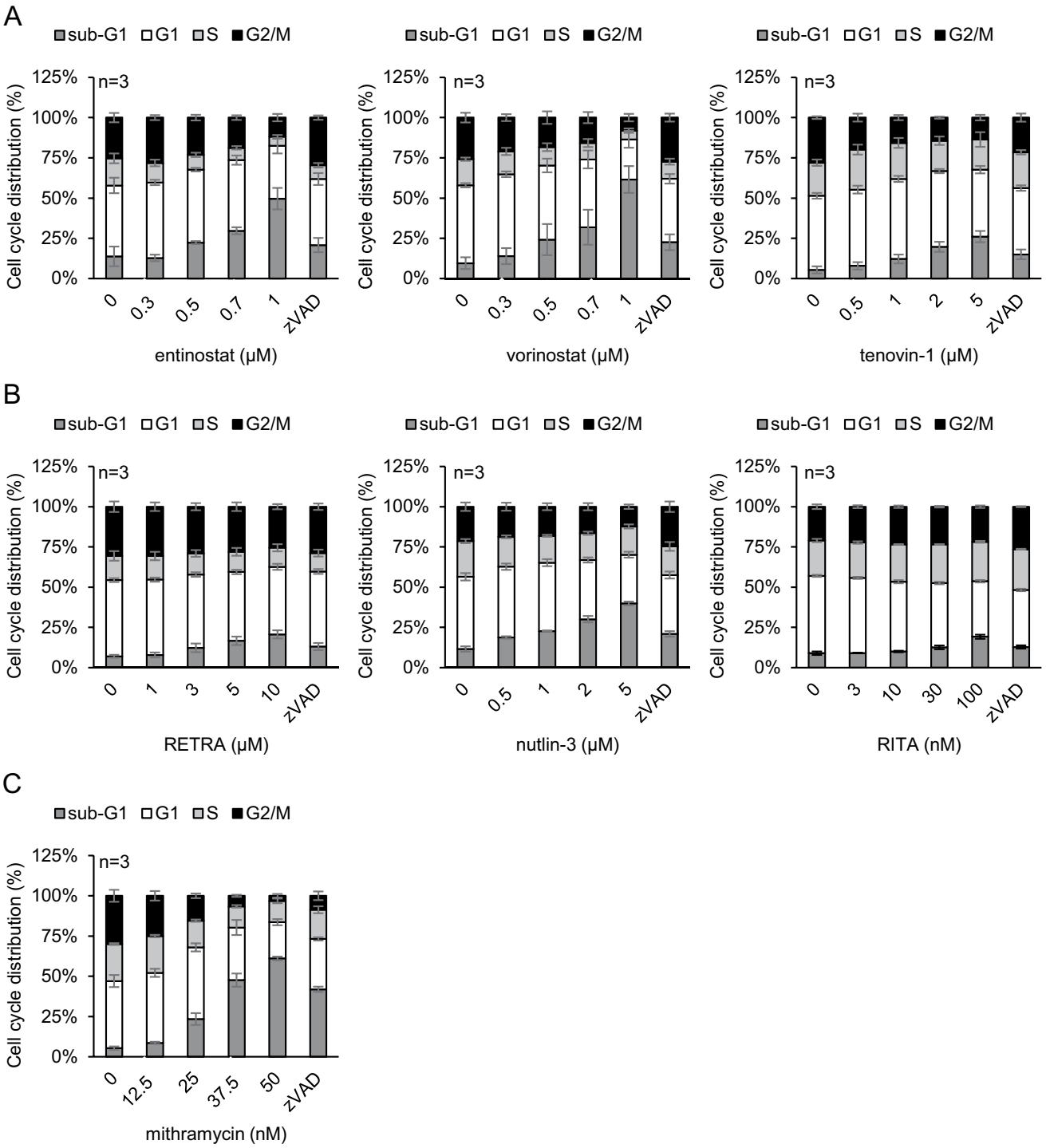


Fig. 3 Cell cycle dynamics and redistribution triggered by target compounds. **A**–**C** Flow cytometric analyses of cell cycle distribution quantifying the percentage of cells in sub-G1, G1, S, and G2/M phases. Cells were analyzed after 48 h exposure to increasing concentrations of: **A** HDACi/SirTi: entinostat, vorinostat and tenovin-1; **B** p53 pathway activators: RETRA, nutlin-3 and RITA; and **C** mithramycin; respective concentrations are depicted in the graph. The rescue effect on cell cycle distribution when the highest applied concentration was combined with 20 μM of zVAD is depicted within the graphs. Accumulation in the sub-G1 fraction marks apoptotic DNA fragmentation. Data are represented as mean ±SEM; the number of replicates is included in the figure

decreased (Fig. 3A). Co-treatment with zVAD decreased the sub-G1 fraction, confirming previous experiments (Figs. 1D and 3A and S6A). To evaluate the upstream activation of p53, expression levels of its targets cyclin-dependent kinase inhibitor p21 (gene name: *CDKN1A*), p53 upregulated modulator of apoptosis (PUMA; gene name: *BBC3*) and NOXA (gene name: *PMAIP1*) (Sullivan et al. 2018; Wang et al. 2021) were assessed by qPCR (Suppl. Fig. S6G). Total RNA was isolated after 24 h treatment with entinostat. This time point precedes the full cytotoxicity that entinostat unfolds at 48 h (Fig. 1C). Treated cells exhibited a 1.7-fold increase in *p21* and *PUMA*, and a 2.5-fold increase in *NOXA* mRNA expression (Suppl. Fig. S6G), showing a weak but notable activation of p53-dependent gene expression in JN-DSRCT-1 cells.

Following treatment with vorinostat, cell cycle analysis tracked a concentration-dependent increase in the sub-G1 fraction at the expense of other phases; however, the relative ratio between G1, S, and G2/M remained uniform, indicating the absence of a true cell cycle arrest (Fig. 3A). As seen with entinostat, co-treatment of vorinostat with zVAD reduced the sub-G1 apoptotic fraction (Fig. 3A). Furthermore, vorinostat induced a 1.5-fold upregulation of *p21* and *NOXA*, and a 1.3-fold increase in *PUMA* mRNA expression (Suppl. Fig. S6G). Cell cycle dynamics showed a concentration-dependent reduction in S and G2/M populations after tenovin-1 treatment, while the G1 fraction remained stable around 46–49% (Fig. 3A). qPCR revealed a strong 3.5-fold upregulation of *p21*, 3-fold increase of *PUMA* and a 1.4-fold increase of *NOXA* mRNA transcripts (Suppl. Fig. S6G), indicating a strong transcriptional activation of p53.

Cell cycle profiling after p53 activation or mithramycin treatment

The p53 signaling (re)activators RETRA, nutlin-3 and RITA induced a uniform, proportional decrease across G1, S, and G2/M-phases shifting cells into the sub-G1 fraction in a concentration-dependent manner, with nutlin-3 showing strongest effects (Fig. 3B). This indicated that RETRA, nutlin-3 or RITA induced apoptosis/cell death rather than an imminent cell cycle arrest. qPCR showed a 1.4-fold increase in *p21* and *PUMA*, and 1.6-fold upregulation of *NOXA* mRNA expression following RETRA treatment and a 2.1-fold increase in *p21*, a 1.9-fold increase in *PUMA*, and 1.2-fold upregulation of *NOXA* mRNA expression following RITA treatment (Suppl. Fig. S6G). Again, nutlin-3 induced the strongest increase in p53-dependent target gene transcription among these three agents: 4-fold in *p21*, 2.7-fold in *PUMA* and 1.4-fold in *NOXA* (Suppl. Fig. S6G).

Mithramycin triggered a robust expansion of the sub-G1 population, which was accompanied by a disproportionately large decline in the G2/M phase compared to the S-phase—indicating a unique disruption of cell cycle distribution (Fig. 3C). While the G1 population remained stable at lower concentrations, it dropped sharply at higher concentrations as the number of sub-G1 cells surged (Fig. 3C). Furthermore, qPCR assays revealed that mithramycin treatment substantially upregulated apoptotic and cell-cycle transcripts, yielding a 2.4-fold increase in *p21*, a 1.9-fold increase in *PUMA*, and a 1.3-fold increase in *NOXA* (Suppl. Fig. S6G), indicating a strong transcriptional activation of p53 comparable to nutlin-3 and tenovin-1.

Discussion

DSRCT is a rare and highly aggressive sarcoma driven by the pathogenic t(11;22)(p13;q12) translocation, which expresses the oncogenic transcription factor EWS-WT1, driving dysregulated gene expression and DSRCT development (Boulay et al. 2024; Gedminas et al. 2020; Hovsepyan et al. 2023; Mello et al. 2021). We characterized the genomic landscape of the JN-DSRCT-1 cell line in detail, performed an in silico analysis of clinical cohort data from DSRCT and ES patients to find vulnerabilities and confirmed the cell line to be a representative and valid model for DSRCT, including chromosomal complexity, key gene alterations and the *EWSR1::WT1* gene fusion. Because intensive multi-agent treatment regimens rarely secure long-term overall patient survival, identifying non-DNA-damaging small-molecule therapies is clinically paramount (Hovsepyan et al. 2023). This study systematically profiled the landscape of promising therapeutics to target the JN-DSRCT-1 cell line, revealing profound sensitivity to epigenetic modifiers alongside direct p53 pathway activators, and the DNA-binding agent mithramycin (Table 1).

Our screening revealed distinct variations in how small molecules effect cell death, highlighting critical therapeutic bottlenecks and resistance mechanisms. The absolute failure of the TKI imatinib to modulate viability aligns with data from DSRCT patients enrolled in clinical trials (Bexelius et al. 2020; Chao et al. 2010). This confirms that DSRCT cell survival depends on deep-seated transcriptional and epigenetic networks rather than upstream surface-receptor tyrosine kinase signaling. In contrast, mithramycin emerged, together with class I/class II HDACi and nutlin-3, as one of the most potent cytotoxic agents in our panel, driving robust cell death at low nanomolar concentrations (Table 1). Since mithramycin binds the minor groove of DNA at GC/GG-rich sequences, it has an influence on different transcription factors, particularly in tumors with deficiencies of the chromatin remodeling SWI/SNF protein complex (Kaufman et al. 2026; Portugal 2024). Thus, mithramycin-induced

Table 1 Summary of small-molecule profiling in the JN-DSRCT-1 cell line

Compound	Effective concentration	Max. cell death	Max. $\Delta\Psi_m$ loss	Caspase−3 induction	zVAD effect	p21 expression
Entinostat	0.3–1.0 µM	~65%	~69%	2.6-fold	yes	1.7-fold
Vorinostat	0.3–1.0 µM	~81%	~85%	4.0-fold	yes	1.5-fold
Tenovin-1	0.5–5.0 µM	~55%	~57%	3.5-fold	no	3.5-fold
RETRA	1–10 µM	~28%	~31%	1.4-fold	no	1.4-fold
Nutlin-3	0.5–5.0 µM	~73%	~72%	4.6-fold	yes	4-fold
RITA	3–100 nM	~46%	~49%	5.4-fold	no	2.1-fold
Mithramycin	12.5–50.0 nM	~80%	~86%	5.4-fold	yes	2.4-fold

chromatin alterations and changes in gene expression patterns might also contribute to in the cytotoxicity of this agent.

The elevated frequency of *ARID1A* and *TP53* mutations in DSRCT (Dermawan et al. 2024) might be a key weakness of this cancer. Among the tested HDACi, we see the high potency of class I/class II HDACs in impacting DSRCT survival, which primarily deacetylate histone proteins and thus, regulate chromatin structures and gene expression patterns (Seto and Yoshida 2014; Thomas et al. 2011). This corresponds to *ARID1A* mutations in DSRCTs and related chromosomal structure alterations, making DSRCTs vulnerable against class I/class II HDACi (Fukumoto et al. 2018a, 2018b; Megino-Luque et al. 2022). EWS-WT1 promotes the activation of the anti-apoptotic, pro-proliferative transcription factors STAT3 and STAT5 in DSCRT cells (Wong et al. 2002). Future studies are necessary to show if the impact of these HDACi on JAK-STAT signaling (Mustafa and Krämer 2023) can explain their toxic effects on such cells. Treatment with classical HDAC inhibitors (entinostat and vorinostat), as well as with nutlin-3, or mithramycin triggered intrinsic apoptosis, characterized by a loss of $\Delta\Psi_m$, caspase−3 activation, and sub-G1 DNA fragmentation. Co-treatment with the pan-caspase inhibitor zVAD significantly reduced overall cell death (Table 1), confirming a caspase-mediated cascade downstream of $\Delta\Psi_m$ loss (Tait and Green 2008).

Conversely, zVAD completely failed to rescue cell viability following treatment with the SirTi tenovin-1, and p53 pathway activators RITA, or RETRA (Table 1). While these compounds strongly activated caspase−3 independently, their cytotoxicity remained unhalted by caspase inhibition, indicating that alternative, programmed necrotic or necroptotic pathways become dominant when intrinsic apoptosis is blocked (Kroemer and Martin 2005; Vandenabeele et al. 2006). Notably, for apoptotic-dominant agents (entinostat, vorinostat, nutlin-3 and mithramycin), the overall percentage of dead cells consistently exceeded the sub-G1 fraction. This decoupling, combined with the fact that zVAD suppressed DNA fragmentation better than total cell death, indicates that a substantial subpopulation of DSRCT cells undergoes parallel, caspase-independent necrosis (Kroemer and Martin 2005; Vandenabeele et al. 2006). P53- and caspase-independent cell death mechanisms in various cancer entities are well documented by our group and involve, for example, apoptosis-inducing factor (AIF) signaling, endoplasmic reticulum stress and autophagy (Gschwind et al. 2022; Marx et al. 2018, 2021; Sonnemann et al. 2015, 2014). Hence, alternative cell death pathways become dominant after caspase inhibition in DSRCT. Relying solely on caspase-dependent mechanisms in the clinic may therefore leave therapies vulnerable to resistance if downstream apoptotic checkpoints mutate.

Cell cycle profiling in this screening showed that p53 pathway activators (RETRA, nutlin-3 and RITA) did not change cell cycle profiles per se, although they increased the sub-G1 fraction of cells. However, the chromatin remodeling HDACi (entinostat and vorinostat) together with the DNA-binding mithramycin induced a concentration-dependent cell cycle arrest in parallel to increased sub-G1 cell fractions. This might be a relevant aspect for designing novel therapies for DSRCT, particularly when combining these agents with classical DNA-damaging chemotherapy or cell cycle inhibitors, such as CDK inhibitors.

The status of p53 and its function in DSRCT has been historically debated; while in silico analysis and sequencing confirmed a high frequency of *TP53* mutations across DSRCT cohorts, our transcriptional profiling indicates that p53 pathways in JN-DSRCT-1 cells remain functional despite two single nucleotide variants of *TP53*. Treatment with HDAC/SirT inhibitors, MDM2 antagonists, and mithramycin uniformly triggered a statistically significant upregulation of the canonical p53 target genes (Sullivan et al. 2018; Wang et al. 2021) *CDKN1A* (p21), *BBC3* (PUMA), and *PMAIP1* (NOXA) prior to structural cell death. Interestingly, tenovin-1, which activates wt-p53 (Lain et al. 2008; Marx et al. 2018; Sonnemann et al. 2014), together with p53 activators (RITA and nutlin-3) and mithramycin induced the strongest increase in p53 target gene transcription (Table 1), potentially eliciting a positive effect on tumor-suppression. In addition, we could show that RETRA, which activates p63 and p73 pathways in cancer cells with mt-p53 (Kravchenko et al. 2008; Sonnemann et al. 2015), is ineffective in JN-DSRCT-1 cells compared to nutlin-3 and RITA (Burmakin et al. 2013; Shen and Maki 2011; Sonnemann et al. 2011; Zhan et al. 2022), which directly activate p53

signaling. This provides clear evidence that DSRC tumors can harbor intact wt-p53 pathways that can be therapeutically exploited.

While our in vitro findings demonstrate clear cytotoxic efficacy for class I/class II HDAC inhibitors, nutlin-3 and mithramycin in DSRCT cells, these responses should be validated in complex physiological environments. In particular, confirming whether single-agent potency translates into sustained tumor regression and acceptable tolerability in vivo represents a critical next step. Evaluating these small-molecule compounds in xenograft models will be essential to establish pharmacodynamic biomarkers, assess off-target toxicities, and determine effective therapeutic windows for clinical translation.

To date, several HDACi have successfully transitioned into clinical practice, including vorinostat, romidepsin, belinostat, panabinostat (no longer FDA approved), givinostat, and chidamide (Iyer et al. a2026; Mustafa and Krämer 2023). Although regulatory approvals vary globally across agencies such as the United States Food and Drug Administration (FDA), European Medicines Agency (EMA), National Medical Products Administration (NMPA) in China and Pharmaceuticals and Medical Devices Agency (PMDA) in Japan, these agents already demonstrate promising therapeutic potential of targeting histone deacetylation in cancer patients (Iyer et al. 2026; Mustafa and Krämer 2023) and might be applied to DSRCT patients in future. From a clinical perspective, despite its universal significance as a tumor suppressor, p53 still remains considered 'undruggable' because restoring mutant protein function presents a greater therapeutic challenge than inhibiting oncogenic activity (Wang et al. 2026). Although various p53 reactivation strategies entered clinical trials over the past decades, none obtained regulatory approval (Wang et al. 2026), reducing their therapeutic potential for DSRCT.

Conclusion

To advance toward biomarker-driven, universally applicable clinical protocols and move away from purely experimental, compassionate-use therapies, the pre-clinical framework must evolve to integrate multi-clonal cellular models in the future. Epigenetic modifiers like entinostat or vorinostat alone or in combination with DNA-binding drugs like mithramycin, classical DNA-damaging chemotherapy or cell cycle inhibitors, such as CDK inhibitors, represents a highly promising, multi-agent strategy to bypass downstream apoptotic resistance, prevent alternative necrotic escape pathways, and effectively eliminate DSRCT.

Limitations

The primary limitation of current pre-clinical DSRCT research is the heavy reliance on a few, long-established cell lines, including JN-DSRCT-1 cells, used as the sole model for the analysis shown in this study. DSRCT is an incredibly heterogeneous disease; individual patient tumors possess unique structural fusion splice variants, varying CNAs, and distinct stromal microenvironments (Boulay et al. 2024; Dermawan et al. 2024), which makes representative in vivo models significantly more difficult to establish. Because DSRCT is rare, clinical trials are virtually impossible to conduct in a prospective, randomized fashion, leaving the oncological community reliant on retrospective analyses (Hovsepyan et al. 2023).

Supplementary Information The online version contains supplementary material available at https://doi.org/10.1007/s00432-026-06630-6.

Acknowledgements The authors like to thank Sigrid Reichard for experimental assistance.

Author contributions A.H. performed the main experimental work and wrote the manuscript. J.H., S.S., S.B. and T.L. per-formed experiments. A.S. supervised the project and wrote the manuscript. O.H.K. and J.S. wrote the manuscript, conceived and supervised the project. C.M. created the images, conceived and wrote the manuscript.

Funding This research was funded by the Thuringian Ministry of Education, Science, and Culture (Nanocellculture FKZ-B714-09064), Federal Ministry of Education and Research (Center of Innovation Competence (FKZ-03ZIK465), (BioLithomorphie FKZ-03Z1M511/512), BloodStemCell Niche FKZ VIP+03VP00591/03VP00592), and the Carl-Zeiss Foundation P2024-02-019. The laboratory of OHK is made possible with funding from the German Research Foundation/Deutsche Forschungsgemeinschaft (DFG) grants KR2291; the Walter Schulz Stiftung; the Brigitte und Dr. Konstanze Wegener-Stiftung (project 110); the Deutsche José Carreras Leukämie-Stiftung (project DJCLS 09 R/204); the H.W. & J. Hector Stiftung (project M 2419); and the Dr. Werner Jackstädt-Stiftung.

Data availability The data that support the findings of this study are available from the corresponding author up-on reasonable request.

Declarations

Conflict of interest The authors declare no conflict of interest.

Consent for publication Not applicable.

Ethical approval Not applicable.

Open Access This article is licensed under a Creative Commons Attribution 4.0 International License, which permits use, sharing, adaptation, distribution and reproduction in any medium or format, as long as you give appropriate credit to the original author(s) and the source, provide a link to the Creative Commons licence, and indicate if changes were made. The images or other third party material in this

article are included in the article's Creative Commons licence, unless indicated otherwise in a credit line to the material. If material is not included in the article's Creative Commons licence and your intended use is not permitted by statutory regulation or exceeds the permitted use, you will need to obtain permission directly from the copyright holder. To view a copy of this licence, visit http://creativecommons.org/licenses/by/4.0/.

References

Abreu RBV, Pereira AS, Rosa MN, Ashton-Prolla P, Silva VAO, Melendez ME, Palmero EI (2024) Functional evaluation of germline *TP53* variants identified in Brazilian families at-risk for Li-Fraumeni syndrome. Sci Rep 14:17187. https://doi.org/10.1038/s41598-024-67810-3

Bexelius TS, Wasti A, Chisholm JC (2020) Mini-review on targeted treatment of desmoplastic small round cell tumor. Front Oncol 10:518. https://doi.org/10.3389/fonc.2020.00518

Boulay G, Broye LC, Dong R, Iyer S, Sanalkumar R, Xing YH, Buisson R, Rengarajan S, Naigles B, Duc B, Volorio A, Awad ME, Renella R, Chebib I, Nielsen GP, Choy E, Cote GM, Zou L, Letovanec I, Stamenkovic I, Rivera MN, Riggi N (2024) EWS-WT1 fusion isoforms establish oncogenic programs and therapeutic vulnerabilities in desmoplastic small round cell tumors. Nat Commun 15:7460. https://doi.org/10.1038/s41467-024-51851-3

Burmakin M, Shi Y, Hedstrom E, Kogner P, Selivanova G (2013) Dual targeting of wild-type and mutant p53 by small molecule RITA results in the inhibition of N-Myc and key survival oncogenes and kills neuroblastoma cells in vivo and in vitro. Clin Cancer Res 19:5092–5103. https://doi.org/10.1158/1078-0432.CCR-12-2211

Campa D, Pastore M, Gentiluomo M, Talar-Wojnarowska R, Kupcinskas J, Malecka-Panas E, Neoptolemos JP, Niesen W, Vodicka P, Delle Fave G, Bueno-de-Mesquita HB, Gazouli M, Pacetti P, Di Leo M, Ito H, Kluter H, Soucek P, Corbo V, Yamao K, Hosono S, Kaaks R, Vashist Y, Gioffreda D, Strobel O, Shimizu Y, Dijk F, Andriulli A, Ivanauskas A, Bugert P, Tavano F, Vodickova L, Zambon CF, Lovecek M, Landi S, Key TJ, Boggi U, Pezzilli R, Jamroziak K, Mohelnikova-Duchonova B, Mambrini A, Bambi F, Busch O, Pazienza V, Valente R, Theodoropoulos GE, Hackert T, Capurso G, Cavestro GM, Pasquali C, Basso D, Sperti C, Matsuo K, Buchler M, Khaw KT, Izbicki J, Costello E, Katzke V, Michalski C, Stepien A, Rizzato C, Canzian F (2016) Functional single nucleotide polymorphisms within the cyclin-dependent kinase inhibitor 2A/2B region affect pancreatic cancer risk. Oncotarget 7:57011–57020. https://doi.org/10.18632/oncotarget.10935

Chao J, Budd GT, Chu P, Frankel P, Garcia D, Junqueira M, Loera S, Somlo G, Sato J, Chow WA (2010) Phase II clinical trial of imatinib mesylate in therapy of KIT and/or PDGFRalpha-expressing Ewing sarcoma family of tumors and desmoplastic small round cell tumors. Anticancer Res 30:547–552

Corless CL, Schroeder A, Griffith D, Town A, McGreevey L, Harrell P, Shiraga S, Bainbridge T, Morich J, Heinrich MC (2005) PDGFRA mutations in gastrointestinal stromal tumors: frequency, spectrum and in vitro sensitivity to imatinib. J Clin Oncol 23:5357–5364. https://doi.org/10.1200/JCO.2005.14.068

Crompton BD, Stewart C, Taylor-Weiner A, Alexe G, Kurek KC, Calicchio ML, Kiezun A, Carter SL, Shukla SA, Mehta SS, Thorner AR, de Torres C, Lavarino C, Sunol M, McKenna A, Sivachenko A, Cibulskis K, Lawrence MS, Stojanov P, Rosenberg M, Ambrogio L, Auclair D, Seepo S, Blumenstiel B, DeFelice M, Imaz-Rosshandler I, Schwarz-Cruz YCA, Rivera MN, Rodriguez-Galindo C, Fleming MD, Golub TR, Getz G, Mora J, Stegmaier K (2014) The genomic landscape of pediatric Ewing sarcoma. Cancer Discov 4:1326–1341. https://doi.org/10.1158/2159-8290.CD-13-1037

Danishevich A, Bilyalov A, Nikolaev S, Khalikov N, Isaeva D, Levina Y, Makarova M, Nemtsova M, Chernevskiy D, Sagaydak O, Baranova E, Vorontsova M, Byakhova M, Semenova A, Galkin V, Khatkov I, Gadzhieva S, Bodunova N (2023) CDKN2A gene mutations: implications for hereditary cancer syndromes. Biomedicines 11:3343. https://doi.org/10.3390/biomedicines11123343

De Souza C, Madden J, Koestler DC, Minn D, Montoya DJ, Minn K, Raetz AG, Zhu Z, Xiao WW, Tahmassebi N, Kathi HR, Nelson N, Karnezis AN, Chien J (2021) Effect of the p53 P72R polymorphism on mutant TP53 allele selection in human cancer. J Natl Cancer Inst 113:1246–1257. https://doi.org/10.1093/jnci/djab019

Delattre O, Zucman J, Plougastel B, Desmaze C, Melot T, Peter M, Kovar H, Joubert I, de Jong P, Rouleau G et al (1992) Gene fusion with an ETS DNA-binding domain caused by chromosome translocation in human tumours. Nature 359:162–165. https://doi.org/10.1038/359162a0

Dermawan JK, Slotkin E, Tap WD, Meyers P, Wexler L, Healey J, Vanoli F, Vanderbilt CM, Antonescu CR (2024) Chromoplexy is a frequent early clonal event in EWSR1-rearranged round cell sarcomas that can be detected using clinically validated targeted sequencing panels. Cancer Res 84:1504–1516. https://doi.org/10.1158/0008-5472.CAN-23-2573

Dho SH, Cho M, Woo W, Jeong S, Kim LK (2025) Caspases as master regulators of programmed cell death: apoptosis, pyroptosis and beyond. Exp Mol Med 57:1121–1132. https://doi.org/10.1038/s12276-025-01470-9

Fontana B, Gallerani G, Salamon I, Pace I, Roncarati R, Ferracin M (2023) ARID1A in cancer: friend or foe? Front Oncol 13:1136248. https://doi.org/10.3389/fonc.2023.1136248

Fukumoto T, Park PH, Wu S, Fatkhutdinov N, Karakashev S, Nacarelli T, Kossenkov AV, Speicher DW, Jean S, Zhang L, Wang TL, Shih IM, Conejo-Garcia JR, Bitler BG, Zhang R (2018a) Repurposing pan-HDAC inhibitors for ARID1A-mutated ovarian cancer. Cell Rep 22:3393–3400. https://doi.org/10.1016/j.celrep.2018.03.019

Fukumoto T, Zhang R, Bitler BG (2018b) Epigenetic inhibitors for the precision treatment of ARID1A-mutant ovarian cancers: what are the next steps? Expert Rev Precis Med Drug Dev 3:233–236. https://doi.org/10.1080/23808993.2018.1503050

Gedminas JM, Chasse MH, McBrairty M, Beddows I, Kitchen-Goosen SM, Grohar PJ (2020) Desmoplastic small round cell tumor is dependent on the EWS-WT1 transcription factor. Oncogenesis 9:41. https://doi.org/10.1038/s41389-020-0224-1

Gerald WL, Rosai J (1989) Case 2. Desmoplastic small cell tumor with divergent differentiation. Pediatr Pathol 9:177–183. https://doi.org/10.3109/15513818909022347

Gschwind A, Marx C, Just MD, Severin P, Behring H, Marx-Blümel L, Becker S, Rothenburger L, Förster M, Beck JF, Sonnemann J (2022) Tight association of autophagy and cell cycle in leukemia cells. Cell Mol Biol Lett 27:32. https://doi.org/10.1186/s11658-022-00334-8

Hentschel J, Rubio I, Eberhart M, Hipler C, Schiefner J, Schubert K, Loncarevic IF, Wittig U, Baniahmad A, von Eggeling F (2011) BCR-ABL- and Ras-independent activation of Raf as a novel mechanism of Imatinib resistance in CML. Int J Oncol 39:585–591. https://doi.org/10.3892/ijo.2011.1062

Hovsepyan S, Giani C, Pasquali S, Di Giannatale A, Chiaravalli S, Colombo C, Orbach D, Bergamaschi L, Vennarini S, Gatz SA, Gasparini P, Berlanga P, Casanova M, Ferrari A (2023) Desmoplastic small round cell tumor: from state of the art to future clinical prospects. Expert Rev Anticancer Ther 23:471–484. https://doi.org/10.1080/14737140.2023.2200171

Iyer KA, Koynova-Tenchov R, Sasso JM, Thite T, Deng Y, Zhou QA (2026) The future of epigenetics: emerging technologies and

clinical applications. ACS Pharmacol Transl Sci 9:506–544. https://doi.org/10.1021/acsptsci.5c00729

Kaufman R, Flores G, Boguslawski EA, Kinn-Gurzo S, Chasse M, Beddows I, Adams M, Stout MC, Gaetano L, Lopez R, Veluvolu S, Fuller A, Kitchen-Goosen SM, Tolstyka ZP, Gedminas JM, Grohar PJ (2026) Mithramycin alters EWS::FLI1 DNA binding and RNA polymerase II processivity to inhibit nascent transcription. Nat Commun 17:2844. https://doi.org/10.1038/s41467-026-69488-9

Kawai-Kawachi A, Lenormand MM, Astier C, Herbel N, Cutrona MB, Ngo C, Garrido M, Eychenne T, Dorvault N, Bordelet L, Song F, Bouyakoub R, Loktev A, Romo-Morales A, Henon C, Colmet-Daage L, Vibert J, Drac M, Brough R, Schwob E, Martella O, Pinna G, Shipley JM, Mittnacht S, Zimmermann A, Gulati A, Mir O, Le Cesne A, Faron M, Honore C, Lord CJ, Chabanon RM, Postel-Vinay S (2025) Replication stress is an actionable genetic vulnerability in desmoplastic small round cell tumors. Cancer Res 85:154–170. https://doi.org/10.1158/0008-5472.CAN-23-3603

Klein AM, Biderman L, Tong D, Alaghebandan B, Plumber SA, Mueller HS, van Vlimmeren A, Katz C, Prives C (2021) MDM2, MDMX, and p73 regulate cell-cycle progression in the absence of wild-type p53. Proc Natl Acad Sci U S A. https://doi.org/10.1073/pnas.2102420118

Koppenhafer SL, Geary EL, Thomas MV, Croushore EE, Zimmerman JAO, Gedminas JM, Quelle DE, Dodd RD, Gordon DJ (2025) Histone deacetylase inhibitors target DNA replication regulators and replication stress in Ewing sarcoma cells. Cancer Res Commun 5:1034–1048. https://doi.org/10.1158/2767-9764.CRC-25-0058

Kravchenko JE, Ilyinskaya GV, Komarov PG, Agapova LS, Kochetkov DV, Strom E, Frolova EI, Kovriga I, Gudkov AV, Feinstein E, Chumakov PM (2008) Small-molecule RETRA suppresses mutant p53-bearing cancer cells through a p73-dependent salvage pathway. Proc Natl Acad Sci U S A 105:6302–6307. https://doi.org/10.1073/pnas.0802091105

Kroemer G, Martin SJ (2005) Caspase-independent cell death. Nat Med 11:725–730. https://doi.org/10.1038/nm1263

Lain S, Hollick JJ, Campbell J, Staples OD, Higgins M, Aoubala M, McCarthy A, Appleyard V, Murray KE, Baker L, Thompson A, Mathers J, Holland SJ, Stark MJ, Pass G, Woods J, Lane DP, Westwood NJ (2008) Discovery, in vivo activity, and mechanism of action of a small-molecule p53 activator. Cancer Cell 13:454–463. https://doi.org/10.1016/j.ccr.2008.03.004

Liang T, Wang F, Elhassan RM, Cheng Y, Tang X, Chen W, Fang H, Hou X (2023) Targeting histone deacetylases for cancer therapy: trends and challenges. Acta Pharm Sin B 13:2425–2463. https://doi.org/10.1016/j.apsb.2023.02.007

Liehr T (2026a) Commercial FISH probes. In: Liehr T (ed) Fluorescence in situ hybridization (FISH): application guide. Springer US, New York, NY, pp 55–67

Liehr T (2026b) Multiplex FISH and spectral karyotyping. In: Liehr T (ed) Fluorescence in situ hybridization (FISH): application guide. Springer US, New York, NY, pp 271–277

Marx C, Marx-Blümel L, Lindig N, Thierbach R, Hoelzer D, Becker S, Wittig S, Lehmann R, Slevogt H, Heinzel T, Wang ZQ, Beck JF, Sonnemann J (2018) The sirtuin 1/2 inhibitor tenovin-1 induces a nonlinear apoptosis-inducing factor-dependent cell death in a p53 null Ewing's sarcoma cell line. Invest New Drugs 36:396–406. https://doi.org/10.1007/s10637-017-0541-1

Marx C, Schaarschmidt MU, Kirkpatrick J, Marx-Blumel L, Halilovic M, Westermann M, Hoelzer D, Meyer FB, Geng Y, Buder K, Schadwinkel HM, Siniuk K, Becker S, Thierbach R, Beck JF, Sonnemann J, Wang ZQ (2021) Cooperative treatment effectiveness of ATR and HSP90 inhibition in Ewing's sarcoma cells. Cell Biosci 11:57. https://doi.org/10.1186/s13578-021-00571-y

Marx-Blümel L, Marx C, Kühne M, Sonnemann J (2017) Assessment of HDACi-induced cytotoxicity. Methods Mol Biol 1510:23–45. https://doi.org/10.1007/978-1-4939-6527-4_3

Megino-Luque C, Siso P, Mota-Martorell N, Navaridas R, de la Rosa I, Urdanibia I, Alberti-Valls M, Santacana M, Pinyol M, Bonifaci N, Macia A, Llobet-Navas D, Gatius S, Matias-Guiu X, Eritja N (2022) ARID1A-deficient cells require HDAC6 for progression of endometrial carcinoma. Mol Oncol 16:2235–2259. https://doi.org/10.1002/1878-0261.13193

Mello CA, Campos FAB, Santos TG, Silva MLG, Torrezan GT, Costa FD, Formiga MN, Nicolau U, Nascimento AG, Silva C, Curado MP, Nakagawa SA, Lopes A, Aguiar S Jr. (2021) Desmoplastic small round cell tumor: a review of main molecular abnormalities and emerging therapy. Cancers (Basel). https://doi.org/10.3390/cancers13030498

Miwa S, Kitamura S, Shirai T, Hayashi K, Nishida H, Takeuchi A, Nojima T, Tsuchiya H (2010) Desmoplastic small round cell tumour successfully treated with caffeine-assisted chemotherapy: a case report and review of the literature. Anticancer Res 30:3769–3774

Mustafa AM, Krämer OH (2023) Pharmacological modulation of the crosstalk between aberrant Janus kinase signaling and epigenetic modifiers of the histone deacetylase family to treat cancer. Pharmacol Rev 75:35–61. https://doi.org/10.1124/pharmrev.122.000612

Nishio J, Iwasaki H, Ishiguro M, Ohjimi Y, Fujita C, Yanai F, Nibu K, Mitsudome A, Kaneko Y, Kikuchi M (2002) Establishment and characterization of a novel human desmoplastic small round cell tumor cell line, JN-DSRCT-1. Lab Invest 82:1175–1182. https://doi.org/10.1097/01.lab.0000028059.92642.03

Portugal J (2024) Mithramycin and its analogs: molecular features and antitumor action. Pharmacol Ther 260:108672. https://doi.org/10.1016/j.pharmthera.2024.108672

Sankar S, Lessnick SL (2011) Promiscuous partnerships in Ewing's sarcoma. Cancer Genet 204:351–365. https://doi.org/10.1016/j.cancergen.2011.07.008

Seto E, Yoshida M (2014) Erasers of histone acetylation: the histone deacetylase enzymes. Cold Spring Harb Perspect Biol 6:a018713. https://doi.org/10.1101/cshperspect.a018713

Shen H, Maki CG (2011) Pharmacologic activation of p53 by small-molecule MDM2 antagonists. Curr Pharm des 17:560–568. https://doi.org/10.2174/138161211795222603

Sonnemann J, Palani CD, Wittig S, Becker S, Eichhorn F, Voigt A, Beck JF (2011) Anticancer effects of the p53 activator nutlin-3 in Ewing's sarcoma cells. Eur J Cancer 47:1432–1441. https://doi.org/10.1016/j.ejca.2011.01.015

Sonnemann J, Marx C, Becker S, Wittig S, Palani CD, Krämer OH, Beck JF (2014) P53-dependent and p53-independent anticancer effects of different histone deacetylase inhibitors. Br J Cancer 110:656–667. https://doi.org/10.1038/bjc.2013.742

Sonnemann J, Grauel D, Blümel L, Hentschel J, Marx C, Blumrich A, Focke K, Becker S, Wittig S, Schinkel S, Krämer OH, Beck JF (2015) RETRA exerts anticancer activity in Ewing's sarcoma cells independent of their TP53 status. Eur J Cancer 51:841–851. https://doi.org/10.1016/j.ejca.2015.02.016

Sullivan KD, Galbraith MD, Andrysik Z, Espinosa JM (2018) Mechanisms of transcriptional regulation by p53. Cell Death Differ 25:133–143. https://doi.org/10.1038/cdd.2017.174

Tait SW, Green DR (2008) Caspase-independent cell death: leaving the set without the final cut. Oncogene 27:6452–6461. https://doi.org/10.1038/onc.2008.311

Thomas S, Miller A, Thurn KT, Munster P (2011) Chapter 37 - clinical applications of histone deacetylase inhibitors. In: Tollefsbol T (ed) Handbook of epigenetics. Academic Press, San Diego, pp 597–615

Tirode F, Surdez D, Ma X, Parker M, Le Deley MC, Bahrami A, Zhang Z, Lapouble E, Grossetete-Lalami S, Rusch M, Reynaud S, Rio-Frio T, Hedlund E, Wu G, Chen X, Pierron G, Oberlin O, Zaidi S, Lemmon G, Gupta P, Vadodaria B, Easton J, Gut M, Ding L, Mardis ER, Wilson RK, Shurtleff S, Laurence V, Michon J, Marec-Berard P, Gut I, Downing J, Dyer M, Zhang J, Delattre O, St. Jude Children's Research Hospital-Washington University Pediatric Cancer Genome P, International Cancer Genome C (2014) Genomic landscape of Ewing sarcoma defines an aggressive subtype with co-association of STAG2 and TP53 mutations. Cancer Discov 4:1342–1353. https://doi.org/10.1158/2159-8290.CD-14-0622

van Kampen F, Clark A, Soul J, Kanhere A, Glenn MA, Pettitt AR, Kalakonda N, Slupsky JR (2025) Deletion of 17p in cancers: guilt by (p53) association. Oncogene 44:637–651. https://doi.org/10.1038/s41388-025-03300-8

Vandenabeele P, Vanden Berghe T, Festjens N (2006) Caspase inhibitors promote alternative cell death pathways. Sci STKE. https://doi.org/10.1126/stke.3582006pe44

Wang J, Thomas HR, Li Z, Yeo NCF, Scott HE, Dang N, Hossain MI, Andrabi SA, Parant JM (2021) Puma, noxa, p53, and p63 differentially mediate stress pathway induced apoptosis. Cell Death Dis 12:659. https://doi.org/10.1038/s41419-021-03902-6

Wang H, Guo M, Wei H, Chen Y (2023) Targeting p53 pathways: mechanisms, structures, and advances in therapy. Signal Transduct Target Ther 8:92. https://doi.org/10.1038/s41392-023-01347-1

Wang W, Liu X, Liu H, Abolhassani H, Yan H, Zhang H, Wang X (2026) p53: from understanding its structure to advances in therapeutic targeting. Signal Transduct Target Ther 11:121. https://doi.org/10.1038/s41392-025-02549-5

Weise A, Liehr T (2026) Pre- and postnatal diagnostics and research on peripheral blood, bone marrow chorion, amniocytes, and fibroblasts. In: Liehr T (ed) Fluorescence in situ hybridization (FISH): application guide. Springer US, New York, NY, pp 187–197

Wolf ER, McAtarsney CP, Bredhold KE, Kline AM, Mayo LD (2018) Mutant and wild-type p53 form complexes with p73 upon phosphorylation by the kinase JNK. Sci Signal 11:eaao4170. https://doi.org/10.1126/scisignal.aao4170

Wong JC, Lee SB, Bell MD, Reynolds PA, Fiore E, Stamenkovic I, Truong V, Oliner JD, Gerald WL, Haber DA (2002) Induction of the interleukin-2/15 receptor beta-chain by the EWS-WT1 translocation product. Oncogene 21:2009–2019. https://doi.org/10.1038/sj.onc.1205262

Wu QJ, Zhang TN, Chen HH, Yu XF, Lv JL, Liu YY, Liu YS, Zheng G, Zhao JQ, Wei YF, Guo JY, Liu FH, Chang Q, Zhang YX, Liu CG, Zhao YH (2022) The sirtuin family in health and disease. Signal Transduct Target Ther 7:402. https://doi.org/10.1038/s41392-022-01257-8

Xia Y, Liu Y, Yang C, Simeone DM, Sun TT, DeGraff DJ, Tang MS, Zhang Y, Wu XR (2021) Dominant role of CDKN2B/p15INK4B of 9p21.3 tumor suppressor hub in inhibition of cell-cycle and glycolysis. Nat Commun 12:2047. https://doi.org/10.1038/s41467-021-22327-5

Zamzami N, Marchetti P, Castedo M, Decaudin D, Macho A, Hirsch T, Susin SA, Petit PX, Mignotte B, Kroemer G (1995) Sequential reduction of mitochondrial transmembrane potential and generation of reactive oxygen species in early programmed cell death. J Exp Med 182:367–377. https://doi.org/10.1084/jem.182.2.367

Zhan Y, Zhou X, Peuget S, Singh M, Peyser BD, Fan Z, Selivanova G (2022) Decreased DNA damage and improved p53 specificity of RITA analogs. Mol Cancer Ther 21:1524–1534. https://doi.org/10.1158/1535-7163.MCT-22-0119

Publisher's Note Springer Nature remains neutral with regard to jurisdictional claims in published maps and institutional affiliations.